

Dynamical behavior of q -deformed logistic map in superior orbit

Renu Badsawal, Sudesh Kumari and Renu Chugh

Abstract. In this paper, we study the q -deformed logistic map in Mann orbit (superior orbit) which is a two-step fixed point iterative algorithm. The main aim of this paper is to investigate the whole dynamical behavior of the proposed map through various techniques such as fixed point and stability approach, time-series analysis, bifurcation plot, Lyapunov exponent and cobweb diagram. We notice that the chaotic behavior of q -deformed logistic map can be controlled by choosing control parameters carefully. The convergence and stability range of the map can be increased substantially. Moreover, with the help of bifurcation diagrams, we prove that the stability performance of this map is larger than that of existing other one dimensional chaotic maps. This map may have better applications than that of classical logistic map in various situations as its stability performance is larger.

Mathematics Subject Classification (2010): 34H10, 37M10, 37B25, 37F45.

Keywords: Logistic map, q -deformation, Mann orbit, time series analysis, bifurcation plot, Lyapunov exponent (LE), cobweb plot.

1. Introduction

Dynamical systems, an interesting branch of mathematics is primarily devoted to the study of procedures in motion. Such procedures take place in various fields such as the motion of the stars and the galaxies in the heaven [11]. In general, the dynamical systems are expressed by differential or difference equations based on the time-varying parameters.

Starting from the work of Lorenz [22] and May [24], more or less, every scientific field has been filled by the concept of nonlinear differential and discrete difference

Received 09 April 2021; Accepted 08 October 2021.

© Studia UBB MATHEMATICA. Published by Babeş-Bolyai University

 This work is licensed under a Creative Commons Attribution-NonCommercial-NoDerivatives 4.0 International License.

equations. One of the popular discrete difference equation is the standard logistic map given by the relation

$$x_{n+1} = \mu x_n(1 - x_n), n = 0, 1, 2, \dots, \quad (1.1)$$

where $x_n \in [0, 1]$ denotes the population at time n and $\mu > 0$ represents the population growth rate.

This population growth model was originally given by P. F. Verhulst in 1845 and 1847 [15]. Nowadays, the logistic map has become a major breakthrough and has found wider applications in many fields such as image encryption in cryptography [9, 16], traffic control [2, 21] and secure communication system [29] etc. For more information about the behavior of dynamical systems one may refer Devaney [11, 10], Holmgren [15], Alligood et al. [1], Ausloos and Dirickx [3], Elagdi [13], Elhadj and Sprott [14], Chugh et al. [8], Diamond [12], Robinson [28], Wiggins [30], Kumari et al. [18, 19, 7, 17, 20] and various other references therein.

Thus the standard logistic map has become most popular nonlinear model which is used to describe various physical and natural systems. Banerjee and Parthasarathy [4] proposed a deformation of this standard logistic map. The resulting map is known as q -deformed logistic map which is given by the following discrete difference equation

$$[x_{n+1}] = \mu[x_n](1 - [x_n]), \quad (1.2)$$

where

$$[x] = \frac{1 - q^x}{1 - q}. \quad (1.3)$$

Here, q is real and $x_n \in [0, 1]$. This q -deformed logistic map is distinct from the standard logistic map.

In the recent past, the q -deformed physical systems have been the subject of enormous research [6]. Along with, the logistic map various other maps such as Henon map [25] and Gaussian Map [26] have also been analyzed using q -deformations. In 2011, Banerjee and Parthasarathy [4] proposed this q -deformation of logistic map, studied about its concavity, non-trivial fixed points and discussed its stability through Lyapunov exponent by changing the parameter q . The stability of this map was also studied in 2015 by Prasad and Katiyar [27]. In 2019, Canovas and Munoz-Guillermo [5] analyzed this map in which topological entropy was also computed to examine the chaos.

In q -deformation, there is some modification in the map in such a way that in the limiting case $q \rightarrow 1$, the modified map (q -deformed logistic map) changes to the original map (classical logistic map). The inspiration for this work comes from the recognition that the original logistic map considers only a saturation effect, that is, an interaction between the population as a whole and a global external constraint. The q -deformation introduces a real-valued parameter q , which models the interaction between individuals in the species - supraunitary q means interindividual competition, while subunitary q leads to cooperation.

Moreover, the Mann orbit models the "inertia" of the system, or the influence of the immediate past on the discrete dynamics. It introduces another parameter, $\alpha \in [0, 1]$, the smaller the value, the larger the inertia. Therefore, in the present paper

we discuss various dynamical properties of the q -deformed logistic map using Mann orbit. The complete paper is divided into four sections. In Section 1, a brief introduction is given. Section 2 includes some basic definitions, results and notations which have been taken into consideration during our analysis. In Section 3, the whole dynamical behavior of the map is investigated. This section is further divided into six subsections which are mainly devoted to the study of this map through fixed point and stability analysis, time-series representation, bifurcation diagrams, Lyapunov exponent, combined bifurcation and Lyapunov exponent analysis and cobweb plots, respectively. In Section 4, we prove the superiority of q -deformed logistic map in superior orbit. At last, the conclusion of the paper is given in Section 5.

2. Preliminaries

In this section, we recollect some basic definitions, results and concepts which have been used in our study.

Definition 2.1. (*Mann iterative algorithm*)[23]: Let X be a non-empty set and $f: X \rightarrow X$ be an operator. Then for an arbitrary point $x_0 \in X$, the sequence $\{x_n\}$ of all iterates, defined by

$$x_{n+1} = (1 - \alpha_n)x_n + \alpha_n f(x_n), \quad (2.1)$$

where $\alpha_n \in [0, 1], n \in N$, is known as Mann iterative algorithm. The sequence $\{x_n\}$ of iterates is also called Mann orbit. Further, for $\alpha_n = 1$, the Mann orbit reduces to the Picard orbit.

Definition 2.2. (*Fixed point*) [10] Let X be a non-empty set and $f: X \rightarrow X$ be an operator. Then, an arbitrary point $x_0 \in X$ is said to be a fixed point for the mapping f if it satisfies $f(x_0) = x_0$.

Definition 2.3. (*Periodic point*) [10] A point x_0 is said to be periodic for a mapping g if it satisfies $g^p(x_0) = x_0$, where p is the least positive integer and denotes the p^{th} iteration. The sequence of p^{th} iterates with initial choice x_0 is called periodic orbit of period- p .

Definition 2.4. (*Lyapunov exponent*)[1]: Let f be the mapping of reals \mathbb{R} . Then, the Lyapunov exponent (LE) of the mapping f for an orbit $\{x_n\}$ is given by

$$\sigma(x_1) = \lim_{n \rightarrow \infty} \frac{1}{n} \sum_{i=1}^n \ln(|f'(x_i)|), \quad (2.2)$$

provided that the limit on R.H.S. exists. Moreover, for $\sigma < 0$, the orbit of the map represents stable behavior and for $\sigma > 0$, the orbit represents unstable behavior.

3. Experimental analysis of q -deformed logistic map via Mann orbit

This entire section deals with an experimental study of the dynamical behavior of q -deformed logistic map using Mann orbit, which has nowadays become a significant

method for the study of various nonlinear maps.

Let us consider, the q -deformed logistic map given by

$$[x_{n+1}] = f(x_n) = \mu \left(\frac{1 - q^{x_n}}{1 - q} \right) \left(1 - \left(\frac{1 - q^{x_n}}{1 - q} \right) \right), \quad (3.1)$$

where $x_n \in [0, 1]$ and q is real.

By definition of Mann orbit (2.1), we have

$$x_{n+1} = (1 - \alpha_n)x_n + \alpha_n(f(x_n)), \quad (3.2)$$

where $x_n \in [0, 1]$ and $\alpha_n \in [0, 1]$.

Using (3.1) in (3.2), we get

$$x_{n+1} = (1 - \alpha_n)x_n + \alpha_n \left[\mu \left(\frac{1 - q^{x_n}}{1 - q} \right) \left(1 - \left(\frac{1 - q^{x_n}}{1 - q} \right) \right) \right], \quad (3.3)$$

where $x_n \in [0, 1]$, $\alpha_n \in [0, 1]$ and q is real.

Further, it is noticed that in case of $\alpha_n = 1$, the system (3.3) reduces to (3.1) and for $\alpha_n = 0$, the system remains unchanged. For the sake of convenience, we take $\alpha_n = \alpha$ and $x_n = x$ throughout this paper. In this way, Eq. (3.3) takes the following form:

$$Q_{\mu,\alpha}(x) = f(x) = (1 - \alpha)x + \alpha \left[\mu \left(\frac{1 - q^x}{1 - q} \right) \left(1 - \left(\frac{1 - q^x}{1 - q} \right) \right) \right], \quad (3.4)$$

Here, α, μ and q are the control parameters. Now, we apply various experimental techniques one by one to describe the complete dynamical behavior of this map by using the matlab software.

3.1. Fixed point and stability analysis of q -deformed logistic map

The fixed points of this map (3.4) can be computed by using the definition (2.2). So, in order to get its fixed points, we have

$$Q_{\mu,\alpha}(x) = x, \\ \text{i.e., } (1 - \alpha)x + \alpha \left[\mu \left(\frac{1 - q^x}{1 - q} \right) \left(1 - \left(\frac{1 - q^x}{1 - q} \right) \right) \right] = x, \quad (3.5)$$

Let $q^x = X$. Then $x \log q = \log X$ and hence $x = \frac{\log X}{\log q}$. Using these in above Eq. (3.5) and after solving it, we obtain

$$(1 - \alpha) \log X + \frac{\alpha \mu \log q (1 - X)(X - q)}{(1 - q)^2} = \log X, \quad (3.6)$$

Being a quadratic equation in X , the Eq. (3.6) has two roots. Out of which $X = 1$ is obvious or trivial root. This implies that one trivial fixed point of q -deformed logistic map in Mann orbit i.e., $Q_{\mu,\alpha}(x)$ is $x = 0$. But it is difficult to calculate the second fixed point because of the nonlinearity of this system. That fixed point depends on the parameters μ and q . To show this, a graphical representation is given in Fig. 1.

Here, the map $Q_{\mu,\alpha}(x)$ is iterated 100 times i.e., we observe 100 numbers of iterations of this map to compute its fixed points (see Table 1) for all $x \in [0, 1]$. One parameter q is taken to be fixed as $q = 0.5$ (some other value can also be taken) throughout our study. In the table, along with fixed points, the maximum value of

parameter μ is also given for which the system remains convergent and stable . Here, the fixed points are computed up to four decimal places by taking the values of μ up to two decimal places.

From Table 1, we observe that the complete dynamical behavior of this map depends on the parameter α . As we decrease the value of α , the system remains stable even for a larger value of μ . Thus, by decreasing the value of parameter α , the range of convergence and stability of $Q_{\mu,\alpha}(x)$ can be increased significantly up to $\mu = 20.81$.

α	Maximum value of μ	
	for convergence	for stability
0.9	3.05	3.92
0.8	3.40	4.39
0.7	3.85	4.96
0.6	4.45	5.48
0.5	5.35	6.18
0.4	6.68	6.78
0.3	8.91	8.92
0.2	12.36	12.36
0.1	20.81	20.81

TABLE 1. Range of convergence and stability of the map $Q_{\mu,\alpha}(x)$

Also, the fixed points exist when the diagonal line $y = x$ intersects the map $Q_{\mu,\alpha}(x)$ as shown in Fig. 1 at points a and b . Here, we have shown the fixed points a and b at $\mu = 3.05$.

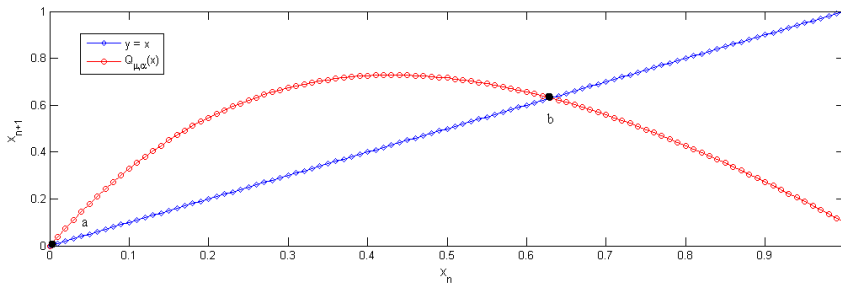


Fig. 1. Graphical representation of fixed points of $Q_{\mu,\alpha}(x)$.

3.2. Time series analysis of q -deformed logistic map for $\alpha = 0.9, 0.5$ and 0.1

In this section, using time series representation of q -deformed logistic map, we try to support the convergence and stability results given in Table 1 graphically. Here, for different values of α against some initial choices of $x \in [0, 1]$, the optimum value of μ is attained by using 100 numbers of iterations.

Example 3.1. Describe the complete dynamical behavior of q -deformed logistic map for $\alpha = 0.9$ and for all $x \in [0, 1]$ by using time series representation of dynamical systems.

Solution. We examine the complete dynamical behavior of q -deformed logistic map for $\alpha = 0.9$ by drawing Figs. 2, 3, 4, 5 and 6. We observe from Fig. 2 that the trajectory of $Q_{\mu,\alpha}(x)$ converges to a fixed point for $0 < \mu \leq 3.05$ for all values of x . This system oscillates between two fixed points for $3.21 < \mu \leq 3.74$ as shown in Fig. 3 at $\mu = 3.5$ for $x_0 = 0.5$. 4-stable oscillations exist for $3.80 < \mu \leq 3.88$ as shown at $\mu = 3.85$ in Fig. 4. The trajectory oscillates between 8-stable fixed points at $\mu = 3.92$ for all $x \in [0, 1]$ as depicted in Fig. 5 for $x_0 = 0.5$. Further, the system starts to show more and more irregular vibrations i.e. sensitive dependence on initials when parameter $\mu \geq 3.93$. This chaoticity of the system is shown at $\mu = 4$ for $x_0 = 0.5$ by Fig. 6.

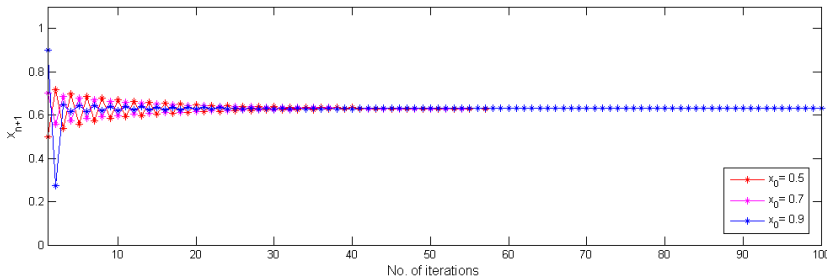


Fig. 2. Stable convergent solution of $Q_{\mu,\alpha}(x)$ for $\alpha = 0.9, \mu = 3.05$

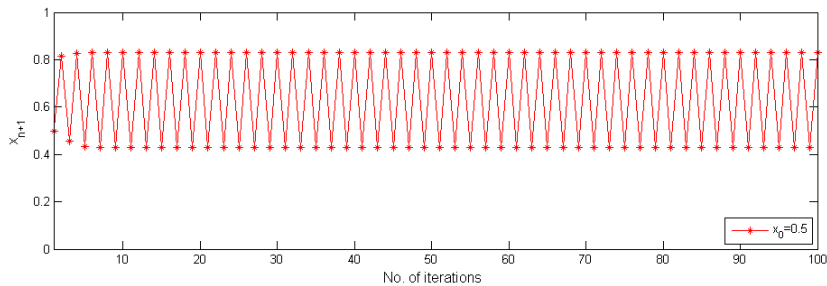


Fig. 3. 2-Stable fixed point oscillation of $Q_{\mu,\alpha}(x)$ for $\alpha = 0.9, \mu = 3.5$

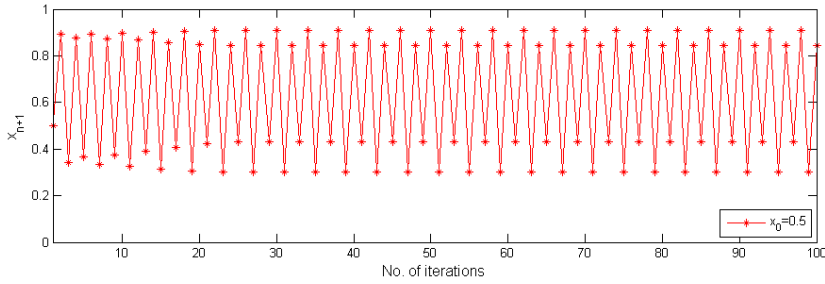


Fig. 4. 4-Stable fixed point oscillation of $Q_{\mu,\alpha}(x)$ for $\alpha = 0.9, \mu = 3.85$

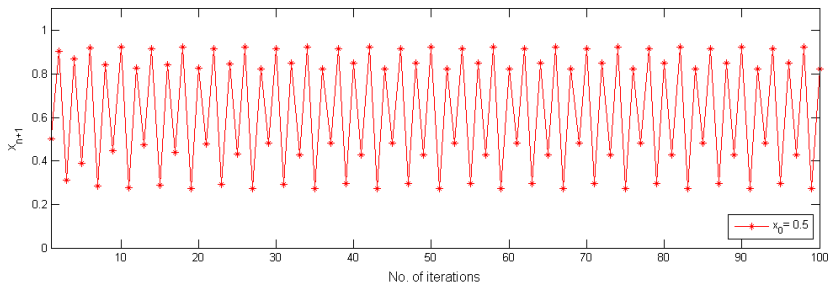


Fig. 5. 8-Stable fixed point oscillation of $Q_{\mu,\alpha}(x)$ for $\alpha = 0.9, \mu = 3.92$

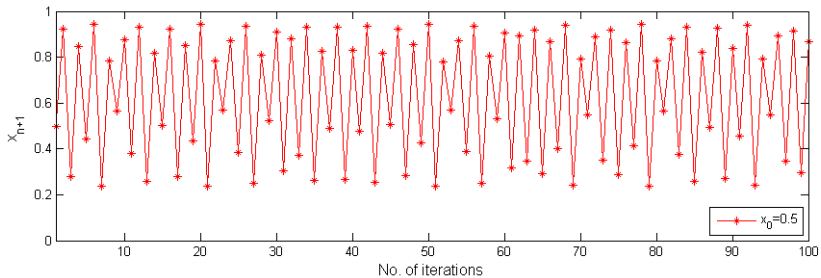


Fig. 6. Divergent behavior of $Q_{\mu,\alpha}(x)$ for $\alpha = 0.9, \mu = 4$

Example 3.2. By using time series analysis, describe the whole dynamical behavior of q -deformed logistic map $Q_{\mu,\alpha}(x)$ for $\alpha = 0.5$ and for all $x \in [0, 1]$ by taking 100 numbers of iterations.

Solution. For this particular value of parameter α , the system has stable fixed point for $0 < \mu \leq 5.35$ for all $x \in [0, 1]$, as shown in Fig. 7 at $x_0 = 0.5$. Also, the trajectory of the system oscillates between two fixed points for $5.63 < \mu \leq 6.18$ and for all $x \in [0, 1]$ as represented in Fig. 8 for $\mu = 6.12$ at $x_0 = 0.5$. Also, for $\mu \geq 6.19$, the system is undefined (see, Fig. 9 for $\mu = 6.19$).

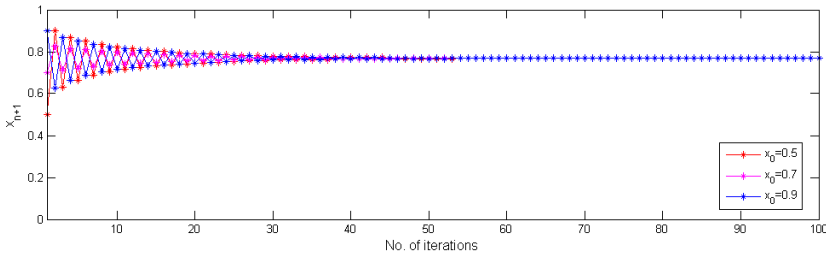


Fig. 7. Stable convergent solution of $Q_{\mu, \alpha}(x)$ for $\alpha = 0.5, \mu = 5.35$

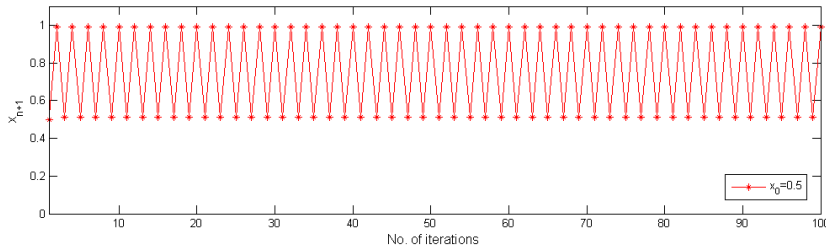


Fig. 8. Stable fixed point oscillation of $Q_{\mu, \alpha}(x)$ for $\alpha = 0.5, \mu = 6.12$

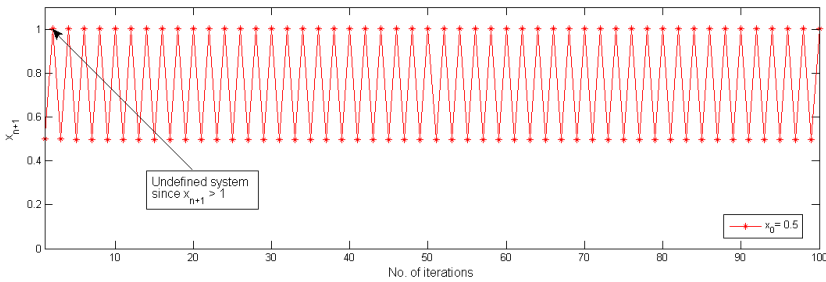


Fig. 9. Undefined $Q_{\mu, \alpha}(x)$ for $\alpha = 0.5, \mu = 6.19$

Example 3.3. Demonstrate that the stability of the map $Q_{\mu, \alpha}(x)$ can be extended by decreasing the value of parameter α . Explain this fact for all $x \in [0, 1]$ by taking $\alpha = 0.1$.

Solution. In this case, the q -deformed map $Q_{\mu, \alpha}(x)$ converges to a stable fixed point for $0 < \mu \leq 20.81$ and for all $x \in [0, 1]$. This convergent behavior is shown in Fig. 10 for $\mu = 20$. In addition, the map $Q_{\mu, \alpha}(x)$ cannot be defined for all $\mu > 20.81$, since in this range $x_{n+1} > 1$ as shown in Fig. 11 for $\mu = 21$ which represents the undefined behavior of the system.

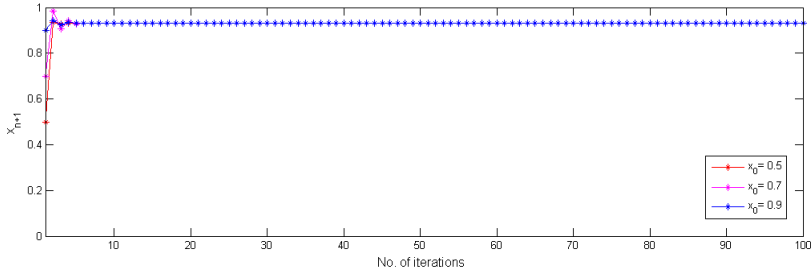


Fig. 10. Stable convergent solution of $Q_{\mu, \alpha}(x)$ for $\alpha = 0.1, \mu = 20$

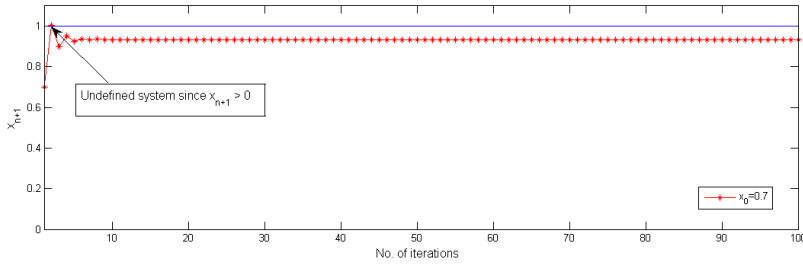


Fig. 11. Undefined $Q_{\mu, \alpha}(x)$ for $\alpha = 0.1, \mu = 21$

3.3. Bifurcation analysis of q -deformed logistic map for different choices of μ

In general, bifurcation diagrams are the tools mainly used to classify the dynamical systems in nonlinear regions. Bifurcation diagrams demonstrate an immediate change that occurs in the asymptotic solutions of a dynamical system.

Under this section, the complete dynamical behavior of $Q_{\mu, \alpha}(x)$ is presented by drawing bifurcation diagrams for $\alpha = 0.9, 0.5$ and 0.1 . A route from periodic region to chaotic region has been shown in Figs. 12, 13, 14 by letting step size for parameter $\mu = 0.001$, initial choice $x_0 = 0.5$ and the number of iterations (N) = 800.

In Fig. 12, the entire dynamical system $Q_{\mu, \alpha}(x)$ has been divided into different regions which explain the complexity of the system. For $0 < \mu \leq 3.15$, the system $Q_{\mu, \alpha}(x)$ has a stable fixed point and period-doubling bifurcation occurs for $3.15 < \mu \leq 3.78$ as shown by regions of period-1 and period-2. Also, the system shows the route from 2-periods to more than 2-periods for $3.78 < \mu \leq 3.95$. The system becomes chaotic as parameter μ exceeds from 3.95, i.e., for $\mu > 3.95$, the system shows sensitive dependence on initials.

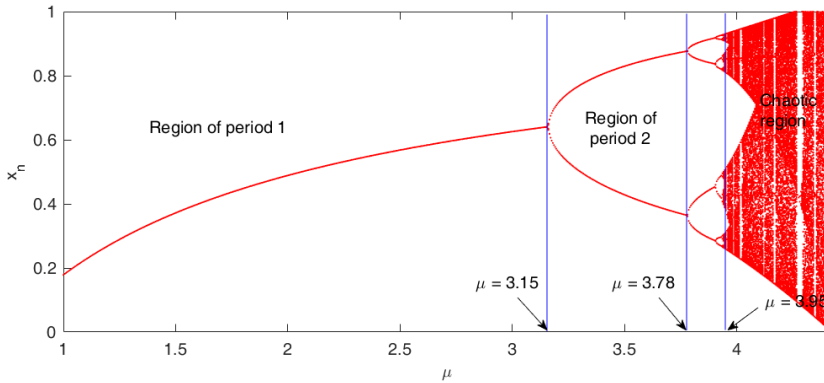


Fig. 12. Bifurcation plot of $Q_{\mu, \alpha}(x)$ for $3 \leq \mu \leq 4, \alpha = 0.9, x_0 = 0.5$

Moreover, period doubling bifurcation for the q -deformed logistic map is represented at $\alpha = 0.5$ in Fig. 13. For this, the system has stable solutions for $0 < \mu \leq 6.18$. Also, the system cannot be defined when the parameter μ exceeds from 6.18 as shown by undefined region.

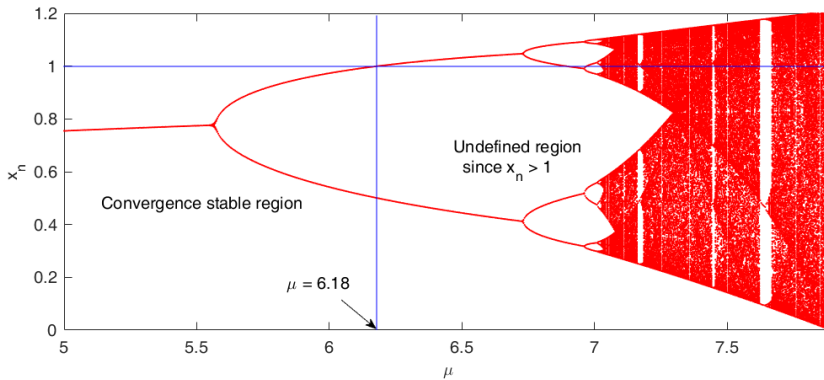


Fig. 13. Bifurcation plot of $Q_{\mu, \alpha}(x)$ for $5 \leq \mu \leq 7.5, \alpha = 0.5, x_0 = 0.5$

Further, from Fig. 14, we observe that the system $Q_{\mu, \alpha}(x)$ remains stable for an extended range of parameter μ , i.e., for $0 < \mu \leq 28.52$, the orbit is convergent to a fixed point. Also, this system cannot be defined for $\mu > 28.52$ as in this range $x_n > 1$. In other words, $x_n \notin [0, 1]$, which represents that the behavior of the system is undefined here.

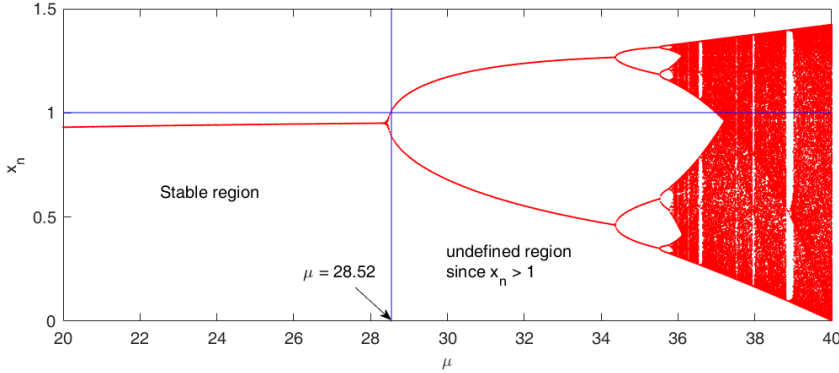


Fig. 14. Bifurcation plot of $Q_{\mu, \alpha}(x)$ for $20 \leq \mu \leq 38$, $\alpha = 0.1$, $x_0 = 0.5$

Remark 1. The system $Q_{\mu, \alpha}(x)$ gains more and more dynamical properties when the value of parameter $\alpha \in [0, 1]$ increases as shown by the bifurcation diagrams, i.e., for $\alpha = 0.1, 0.5$, the system demonstrates fixed point and periodic properties; for $\alpha = 0.9$, system exhibits fixed points, periodicity and chaos.

3.4. Mathematical and experimental analysis of q -deformed logistic map by Lyapunov exponent

An another major characteristic of nonlinear dynamical systems is Lyapunov exponent, which determines the sensitive dependence of two distinct orbits beginning from very close initial positions. In case of stable periodic behavior, the rate of onvergence to stable point is determined by LE, whereas, in case of chaotic behavior, LE determines the rate of divergence between the orbits. For the q -deformed logistic map with Mann iteration ($Q_{\mu, \alpha}(x)$), Lyapunov exponent is defined as follows:

Let us begin the method by taking Mann orbits for two distinct initial choices x and $x + h$, where $0 < h < 1$. Here, Δ represents the divergence between these orbits, which is taken as the exponential growth $he^{n\sigma}$, where σ denotes the Lyapunov exponent of the map and n stands for the number of iterations. So, it can be written as

$$\begin{aligned} Q_{\mu, \alpha}^n(x + h) - Q_{\mu, \alpha}^n(x) &= \Delta \\ Q_{\mu, \alpha}^n(x + h) - Q_{\mu, \alpha}^n(x) &= he^{n\sigma} \\ \therefore \frac{Q_{\mu, \alpha}^n(x + h) - Q_{\mu, \alpha}^n(x)}{h} &= e^{n\sigma}. \end{aligned} \quad (3.7)$$

Taking limit $h \rightarrow 0$, on both sides, we get

$$\begin{aligned} \lim_{h \rightarrow 0} \frac{Q_{\mu, \alpha}^n(x + h) - Q_{\mu, \alpha}^n(x)}{h} &= e^{n\sigma} \\ \text{i.e., } (Q_{\mu, \alpha}^n)'(x) &= e^{n\sigma}. \end{aligned} \quad (3.8)$$

Applying logarithm on both sides, we obtain

$$\sigma = \frac{1}{n} \log |(Q_{\mu,\alpha}^n)'(x)|, \quad (3.9)$$

where $(Q_{\mu,\alpha}^n)'(x)$ represents the first order derivative for the map $Q_{\mu,\alpha}(x)$. For n th degree polynomial, the derivative can be evaluated by applying the chain rule of differentiation.

So, for the succession $x_1, x_2 = Q_{\mu,\alpha}(x_1), x_3 = Q_{\mu,\alpha}(x_2), \dots, x_{n+1} = Q_{\mu,\alpha}(x_n), \dots$, we have

$$(Q_{\mu,\alpha}^n)'(x_1) = Q'_{\mu,\alpha}(x_n) \cdot Q'_{\mu,\alpha}(x_{n-1}) \cdots Q'_{\mu,\alpha}(x_2) \cdot Q'_{\mu,\alpha}(x_1). \quad (3.10)$$

Now, using (3.10) in (3.9), we get

$$\begin{aligned} \sigma &= \frac{1}{n} \log |Q'_{\mu,\alpha}(x_n) \cdot Q'_{\mu,\alpha}(x_{n-1}) \cdots Q'_{\mu,\alpha}(x_2) \cdot Q'_{\mu,\alpha}(x_1)|, \\ &= \frac{1}{n} [\log |Q'_{\mu,\alpha}(x_n)| + \log |Q'_{\mu,\alpha}(x_{n-1})| + \cdots + \log |Q'_{\mu,\alpha}(x_2)| + \log |Q'_{\mu,\alpha}(x_1)|], \\ & \qquad \qquad \qquad \sigma = \frac{1}{n} \sum_{j=1}^n \log |Q'_{\mu,\alpha}(x_j)|, \end{aligned} \quad (3.11)$$

which is the required Lyapunov exponent of $Q_{\mu,\alpha}(x)$.

In addition, if the map has fixed orbit, then (3.11) reduces to

$$\sigma = \ln(|Q'_{\mu,\alpha}(x_1)|). \quad (3.12)$$

Also, for perodic orbit of period- p , we get from (3.11)

$$\sigma = \frac{1}{p} \sum_{j=1}^p \ln(|Q'_{\mu,\alpha}(x_j)|). \quad (3.13)$$

Remark 2. In order to evaluate the Lyapunov exponent for aperiodic orbits, it is almost impossible to utilize the entire length of an orbit. So, only finite length of an orbit is used frequently to estimate the Lyapunov exponent.

Remark 3. Moreover, the fixed and periodic orbits of the map represent stable behavior for $\sigma < 0$ and unstable behavior for $\sigma > 0$. In this way, the Lyapunov exponent demonstrates the stable and unstable nature of various fixed and periodic orbits.

Example 3.4. Calculate the Lyapunov exponent of the map $Q_{\mu,\alpha}(x)$ for the following values of parameters α and μ :

(a) $\alpha = 0.9, \mu = 3$

(b) $\alpha = 0.9, \mu = 3.5$.

Also, examine the dynamical behavior of this map by plotting the Lyapunov exponent for $\alpha = 0.9, 1 \leq \mu \leq 4.4$.

Solution. (a) As discussed in Section 3.2, for $0 < \mu \leq 3.05$, the map $Q_{\mu,\alpha}(x)$ has a fixed orbit for all $x \in [0, 1]$. Also, the fixed point of the orbit for $\mu = 3$ is given as

0.6255. So, to compute the Lyapunov exponent of this orbit, it is enough to solve Eq. (3.12). For that, we have

$$Q_{\mu,\alpha}(x) = (1 - \alpha)x + \alpha \left[\mu \left(\frac{1 - q^x}{1 - q} \right) \left(1 - \left(\frac{1 - q^x}{1 - q} \right) \right) \right],$$

$$Q'_{\mu,\alpha}(x) = (1 - \alpha) + \frac{\alpha\mu}{1 - q} \cdot q^x \cdot \ln q \left[2 \left(\frac{1 - q^x}{1 - q} \right) - 1 \right]. \quad (3.14)$$

Putting $\alpha = 0.9, \mu = 3, x = 0.6255$ in Eq. (3.14), we get

$$Q'_{3,0.9}(0.6255) = -0.3292. \quad (3.15)$$

Now, using (3.15) in (3.12), we obtain

$$\sigma = \ln(| - 0.3292|) = -0.4825.$$

So, the Lyapunov exponent at $\mu = 3$ is -0.4825, which is a negative value and thus from the definition of Lyapunov exponent, this fixed point is a stable attractor.

(b) For $3.21 < \mu \leq 3.74$, the map $Q_{\mu,\alpha}(x)$ represents periodic orbit of period-2 for all $x \in [0, 1]$. So, for $\mu = 3.5$, the periodic points are $x_1 = 0.4281$ nad $x_2 = 0.8297$. Thus, we get

$$Q'_{\mu,\alpha}(x_1) = 0.0617 \quad (3.16)$$

$$Q'_{\mu,\alpha}(x_2) = -0.6997. \quad (3.17)$$

Now, using Eqs. (3.16) and (3.17) in (3.13), we get

$$\begin{aligned} \sigma &= \frac{1}{2} [\ln |Q'_{\mu,\alpha}(x_1)| + \ln |Q'_{\mu,\alpha}(x_2)|] \\ &= \frac{1}{2} [\ln |0.0617| + \ln | - 0.6997|] \\ &= \frac{1}{2} [(-1.2097) + (-0.1551)]. \end{aligned}$$

This gives

$$\sigma = -0.6824$$

So, the Lyapunov exponent is less than zero in this case also. Thus, these periodic points are stable attractors.

In Fig. 15, we plot Lyapunov exponent (σ) to discover the behavior of dynamical system $Q_{\mu,\alpha}(x)$ for $1 \leq \mu \leq 4.4$ at $\alpha = 0.9$. To plot this, we consider 10,000 iterations, i.e., $N = 10,000$ and initiator $x_0 = 0.5$. It is clear from the figure that the system remains stable for $0 < \mu \leq 3.95$ since in this range $\sigma < 0$, i.e., the system preserves stable orbits, Also, in the zoomed rectangular area, the chaotic behavior of the system is represented since here, $\sigma > 0$, i.e., the orbit shows sensitive dependence on initiators. Hence, chaos occurs in the system as we increase the parameter μ from $\mu = 3.95$.

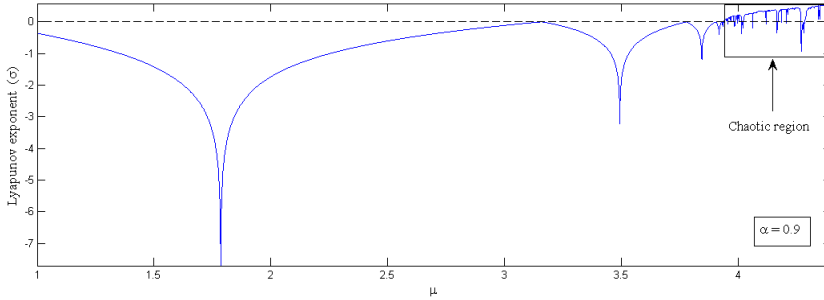


Fig. 15. Lyapunov exponent plot of $Q_{\mu,\alpha}(x)$ for $1 \leq \mu \leq 4.4, \alpha = 0.9, x_0 = 0.5$

Example 3.5. Explain the dynamical behavior of this q -deformed logistic map $Q_{\mu,\alpha}(x)$ by plotting the Lyapunov exponent for the following values of parameters μ and α :

- (a) $1 \leq \mu \leq 7.9, \alpha = 0.5,$
- (b) $1 \leq \mu \leq 28.52, \alpha = 0.1.$

Solution. (a) We investigate the dynamical behavior of $Q_{\mu,\alpha}(x)$ by drawing the Lyapunov exponent diagram as shown in Fig. 16, for the given values of parameters and initiator $x_0 = 0.5$. We observe that the Lyapunov exponent is negative, i.e. $\sigma < 0$ for $0 < \mu \leq 7.07$, which represents the stable behavior of the system. Also for $7.07 < \mu \leq 7.9$, the spectrum of Lyapunov exponent begins to approach a positive value of σ , which indicates that there is chaos in the dynamical system.

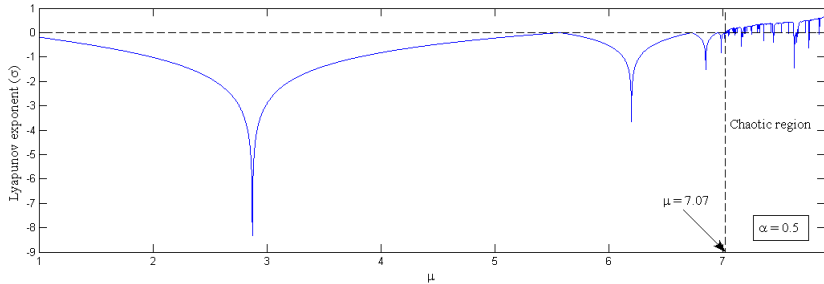


Fig. 16. Lyapunov exponent plot of $Q_{\mu,\alpha}(x)$ for $1 \leq \mu \leq 7.9, \alpha = 0.5, x_0 = 0.5$

(b) The stability of dynamical system can be increased by controlling the parameters. This fact is analyzed here by estimating the value of LE (σ) at a decreased value of parameter α , i.e., at $\alpha = 0.1$. For this particular value of α , the system shows stable behavior for an increased value of parameter μ , i.e., for $0 < \mu \leq 28.52$. We have explained this fact experimentally in Fig. 17. We observe that for $0 < \mu \leq 28.52$, the value of Lyapunov exponent (σ) is negative. Thus the system shows fixed stable behavior for this extended range of μ .

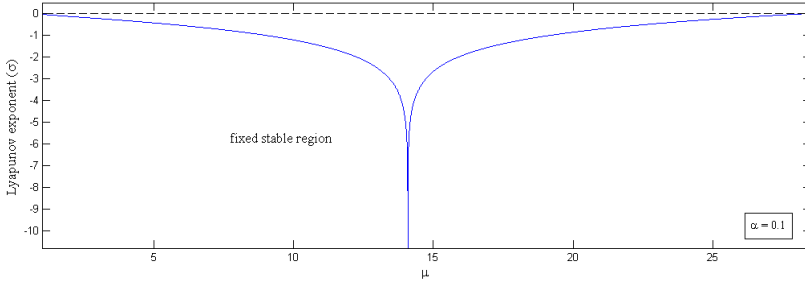


Fig. 17. Lyapunov exponent plot of $Q_{\mu,\alpha}(x)$ for $1 \leq \mu \leq 28.52, \alpha = 0.1, x_0 = 0.5$

3.5. A new experimental analysis of q -deformed logistic map via combined study of bifurcation and Lyapunov exponent

Under this section, we try to investigate the complex dynamical behavior of this system $Q_{\mu,\alpha}(x)$ with the help of combined bifurcation and Lyapunov exponent plots. This experimental technique enables us to investigate the exact value of parameter μ obtained in previous subsections at which the system changes its behavior. In these figures, the entire region of the dynamical system $Q_{\mu,\alpha}(x)$ is divided into distinct regions separated by a magenta dotted line.

Fig. 18 exhibits the combined representation of bifurcation and Lyapunov exponent for $1 \leq \mu \leq 4.4$ at $\alpha = 0.9$. Here, the system has two regions, stable periodic region and chaotic region, separated by a magenta dotted line at $\mu = 3.95$, which is the highest value of μ for which the system remains stable, afterwards chaos occurs.

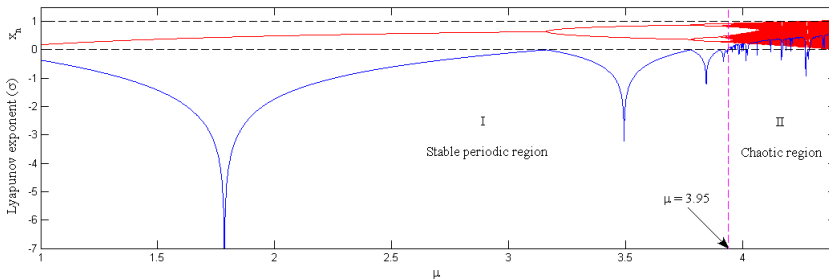


Fig. 18. Bifurcation plot v/s Lyapunov exponent plot of $Q_{\mu,\alpha}(x)$ for $1 \leq \mu \leq 4.4$ at $\alpha = 0.9$

The entire region of $Q_{\mu,\alpha}(x)$ is divided into three regions (stable, undefined and chaotic region) at particular values of parameter μ as shown in Figs. 19 and 20 for $\alpha = 0.5$ and $\alpha = 0.1$ respectively. Also, it can be noticed from the figures that the system preserves its stability for a larger value of parameter μ as we decrease the value of parameter α . Moreover, when $\sigma > 0$, the system represents chaotic behavior.

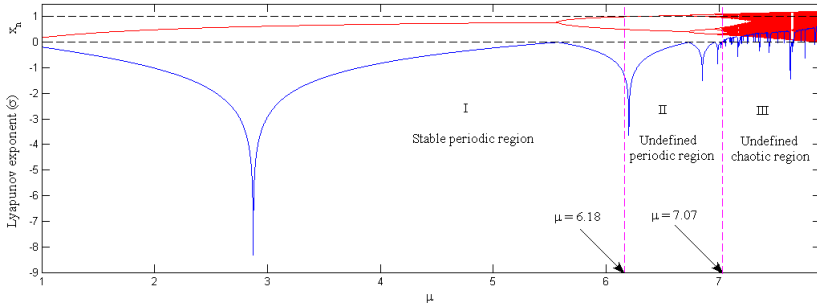


Fig. 19. Bifurcation plot v/s Lyapunov exponent plot of $Q_{\mu, \alpha}(x)$ for $1 \leq \mu \leq 7.9$ at $\alpha = 0.5$

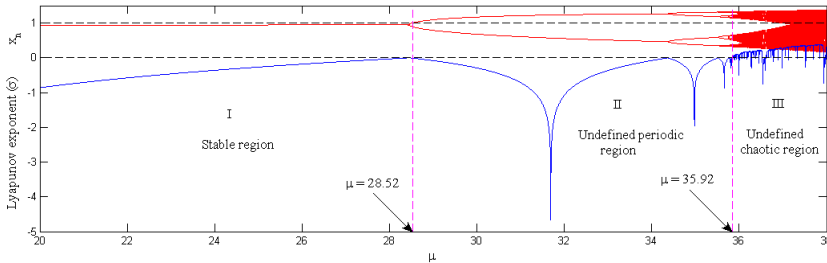


Fig. 20. Bifurcation plot v/s Lyapunov exponent plot of $Q_{\mu, \alpha}(x)$ for $20 \leq \mu \leq 38$ at $\alpha = 0.1$

3.6. Experimental analysis of q -deformed logistic map through cobweb plot

A cobweb diagram is generally a visual method which is used to examine the qualitative nature of the map in the field of dynamical systems. With the help of cobweb plot, we can predict the long term behavior of an initial condition under repeated application of a map.

Fig. 21 depicts the attracting behavior of the fixed point 0.6304 of the map $Q_{\mu, \alpha}(x)$ for the parameters $\alpha = 0.9, \mu = 3.05$ and for initiator $x_0 = 0.5$. Also, the periodic behavior of $Q_{\mu, \alpha}(x)$ for $\alpha = 0.9, \mu = 3.5$ and $x_0 = 0.5$ is shown in Fig. 22. In addition, Fig. 23 represents the unstable behavior of this map for $\alpha = 0.9, \mu = 4, x_0 = 0.5$.

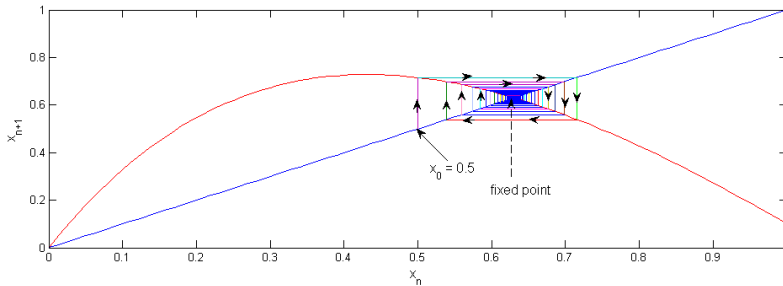


Fig. 21. Attracting behavior of fixed point of $Q_{\mu, \alpha}(x)$ for $\alpha = 0.9, \mu = 3.05$

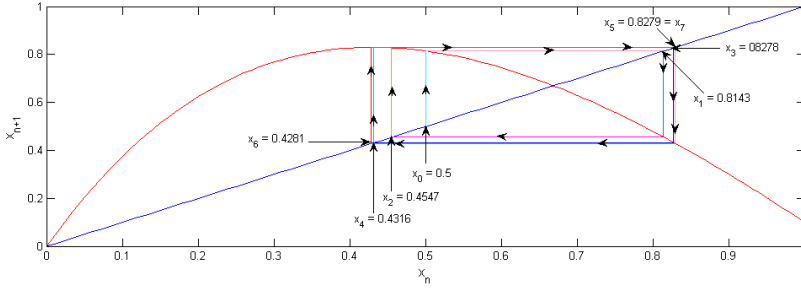


Fig. 22. Periodic behavior of $Q_{\mu,\alpha}(x)$ for $\alpha = 0.9, \mu = 3.5$

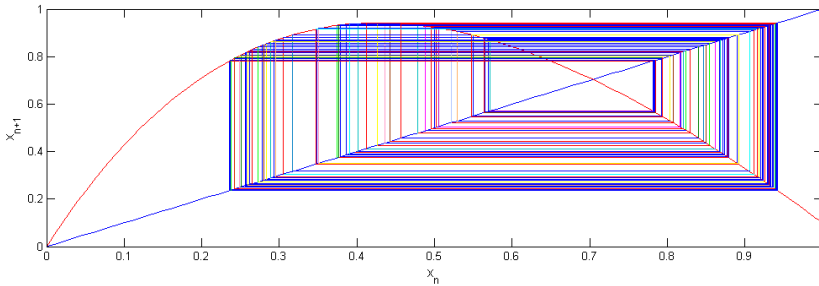


Fig. 23. Unstable behavior of $Q_{\mu,\alpha}(x)$ for $\alpha = 0.9, \mu = 4$

Further, the attracting nature of fixed point 0.7686 for $\alpha = 0.5, \mu = 5.35$ and periodic nature for $\alpha = 0.5, \mu = 5.65$ of the q -deformed map $Q_{\mu,\alpha}(x)$ with initiator $x_0 = 0.5$ are represented in Figs. 24 and 25 respectively.

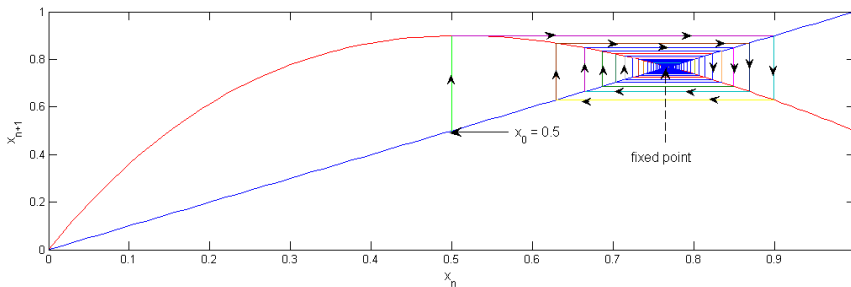


Fig. 24. Attracting behavior of fixed point of $Q_{\mu,\alpha}(x)$ for $\alpha = 0.5, \mu = 5.35$

Moreover, Fig. 26 depicts the attracting behavior of the fixed point 0.9310 of this map $Q_{\mu,\alpha}(x)$ for the parameters $\alpha = 0.1, \mu = 20$ and $x_0 = 0.5$. Also, it is clear from the Fig. 27 that this q -deformed logistic map $Q_{\mu,\alpha}(x)$ is not defined for $\alpha = 0.1, \mu = 21$ and $x_0 = 0.5$, since $x_{n+1} > 1$ here.

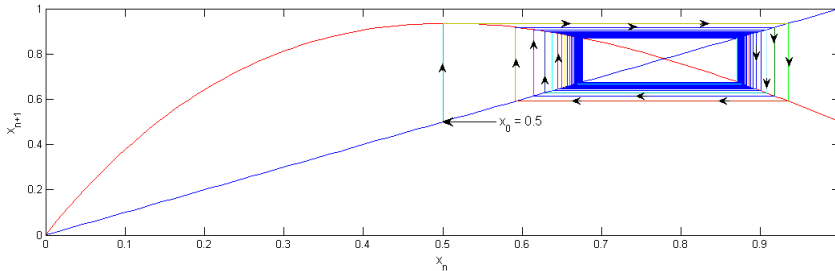


Fig. 25. Periodic behavior of $Q_{\mu,\alpha}(x)$ for $\alpha = 0.5, \mu = 5.65$

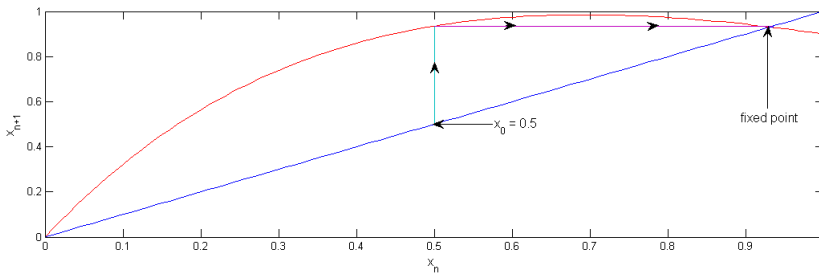


Fig. 26. Attracting behavior of fixed point of $Q_{\mu,\alpha}(x)$ for $\alpha = 0.1, \mu = 20$

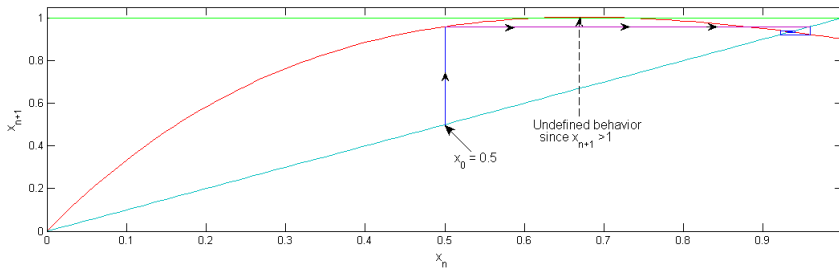


Fig. 27. Undefined behavior of $Q_{\mu,\alpha}(x)$ for $\alpha = 0.1, \mu = 21$

4. Superiority of q -deformed map in superior orbit

To prove the superiority of q -deformed map in superior orbit (3.3), we compare its stability performance with existing one dimensional maps using bifurcation plots.

4.1. Stability performance of q -deformed logistic map in superior orbit

In order to facilitate comparison, we compare the stability performance of the map (3.3) with existing one dimensional maps including classical logistic map, logistic map in superior orbit, sine map and q -deformed logistic map (3.1).

From Fig. 28, we observe that q -deformed logistic map considered in superior orbit (3.3) remains stable for $0 < \mu \leq 28.51$ which we have already shown in Subsection 3.3. In Subfigures 28a - 28d, we draw the bifurcation diagrams to study the stability performance of existing one dimensional chaotic maps. We notice that the classical

logistic map is stable for $0 < \lambda \leq 3.57$ while logistic map in superior orbit remains stable for $0 < \mu \leq 21.2$. Also, the sine map shows its stable behavior for $0 < \mu \leq 0.86$ and the one dimensional q -deformed logistic map attains its stability performance for $0 < \mu \leq 3.58$. This proves that q -deformed logistic map in superior orbit has largest range of stability which is very higher than the existing other one dimensional chaotic maps.

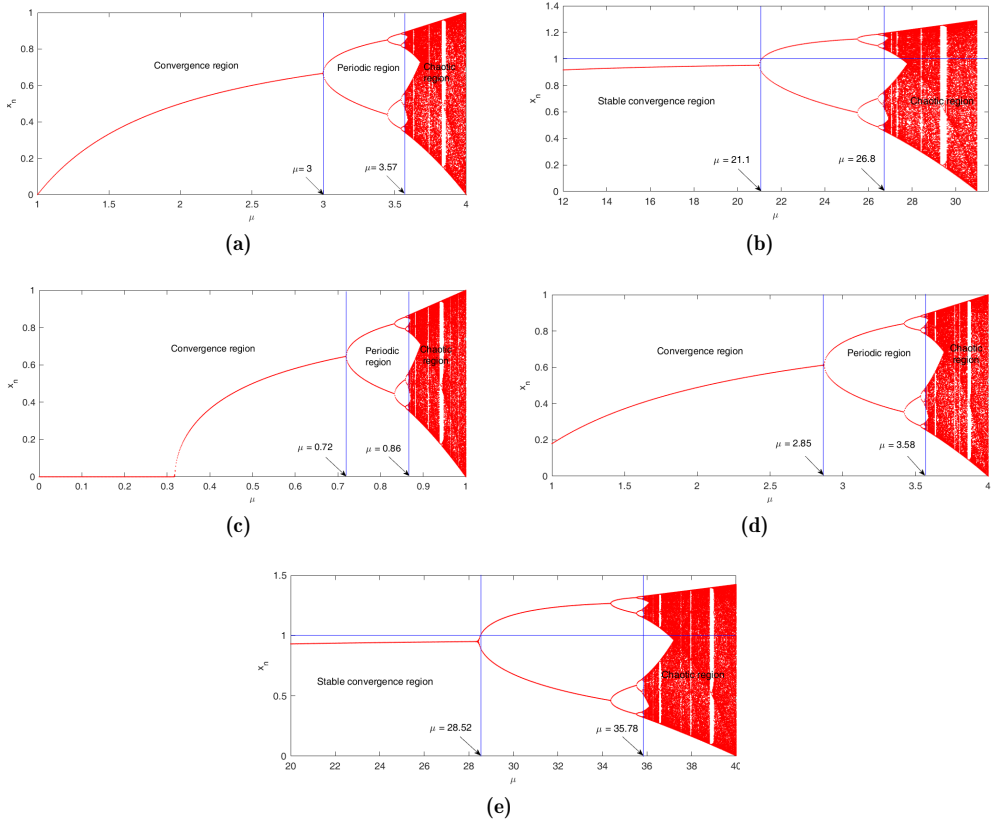


Fig. 28. Bifurcation plots (a) logistic map (b) logistic map in superior orbit (c) sine map (d) q -deformed logistic map and (e) q -deformed logistic map in superior orbit.

5. Conclusion

Here, a novel study of dynamical behavior of the q -deformed logistic map using Mann iterative algorithm is given. In this system, there are three control parameters denoted by α , μ and q . And it is quite interesting to notice that the entire dynamical behavior of this map depends on these three parameters. The q -deformed logistic map is studied via fixed point and stability analysis, time series representation, bifurcation

analysis, Lyapunov exponent method, combined bifurcation and Lyapunov exponent analysis and cobweb plot. The following concluding remarks are drawn from our study:

1. The fixed point analysis approach has been used to compute the fixed points of the system (3.4). Also, the stability performance of the unrestricted system has been checked. The convergence and stability range of the q -deformed logistic map can be increased by choosing the parameters (μ, α) carefully (see, Table 1).
2. The complex dynamical behavior of this q -deformed logistic map has been further examined graphically by using time series representation for $\alpha = 0.9, 0.5$ and 0.1 to confirm the stability results obtained by fixed point analysis.
3. The bifurcation analysis is also used to investigate the various dynamical properties of the map such as fixed point, periodicity and chaos for different choices of μ .
4. The irregular behavior of dynamical system has also been analyzed numerically and experimentally by adopting Lyapunov exponent approach. Furthermore, combined bifurcation and Lyapunov exponent plots are shown to demonstrate various regions of this system. Also, cobweb plots have been used for further investigation.
5. It is strongly highlighted that the q -deformed logistic map has more stability performance than that of existing other one dimensional dynamical systems (see, Fig. 28).
6. For future research, an exhaustive search of the (μ, α) plane, followed by a graphical depiction of the $Q_{\mu, \alpha}(x)$, demarcating the areas of convergence, stability and sensitive dependence might be very interesting.

References

- [1] Alligood, K.T., Sauer, T.D., Yorke, J.A., *Chaos: An Introduction to Dynamical Systems*, Springer, New York, 1996.
- [2] Ashish, C.J., Chugh, R., *Chaotic behavior of logistic map in superior orbit and an improved chaos based traffic control model*, Nonlinear Dynamics, **94**(02)(2018), 959-975.
- [3] Ausloos, M., Dirickx, M., *The Logistic Map and the Route to Chaos: From the Beginnings to Modern Applications*, Springer, New York, 2006.
- [4] Banerjee, S., Parthasarathy, R., *A q -deformed logistic map and its implications*, J. Phys., **44**(2011), no. 4, 04510.
- [5] Canovas, J., Munoz-Guillermo, M., *On the dynamics of q -deformed logistic map*, Phys. Lett. A, **383**(2019), no. 15, 1742-1754.
- [6] Chaichian, M., Demichev, A., *Introduction to Quantum Groups*, World Scientific, Singapore, 1996.
- [7] Chugh, R., Kumar, A., Kumari, S., *A novel epidemic model to analyze and control the chaotic behavior of covid-19 outbreak*, Bull. Transilv. Univ. Braşov, Ser. III, Math. Comput. Sci., **13**(62)(2021), no. 2, 479-508.
- [8] Chugh, R., Rani, M., Ashish, *Logistic map in Noor orbit*, Chaos Complex Lett., **6**(2012), no. 3, 167-175.
- [9] Chunyan, H., *An image encryption algorithm based on modified logistic chaotic map*, Optik, **181**(2019), 779-785.

- [10] Devaney, R.L., *An Introduction to Chaotic Dynamical Systems*, 2nd ed. Addison-Wesley, Boston, 1948.
- [11] Devaney, R.L., *A First Course in Chaotic Dynamical Systems: Theory and Experiment*, Addison-Wesley, Boston, 1992.
- [12] Diamond, P., *Chaotic behaviour of systems of difference equations*, Int. J. Syst. Sci., **7**(1976), no. 8, 953-956.
- [13] Elagdi, S.N., *Chaos: An Introduction to Difference Equations*, Springer, New York, 1999.
- [14] Elhadj, Z., Sprott, J.C., *The effect of modulating a parameter in the logistic map*, Chaos, **18**(2008), no. 2, 1-7.
- [15] Holmgren, R.A., *A First Course in Discrete Dynamical Systems*, Springer, New York, 1994.
- [16] Kumar, S., Kumar, M., Budhiraja, R., Das, M.K., Singh, S., *A secured cryptographic model using intertwining logistic map*, Procedia Computer Science, **143**(2018), 804-811.
- [17] Kumari, S., Chugh, R., *A new experiment with the convergence and stability of logistic map via sp orbit*, Int. J. Appl. Eng. Res., **14**(2019), 797-801.
- [18] Kumari, S., Chugh, R., *A novel four-step feedback procedure for rapid control of chaotic behavior of the logistic map and unstable traffic on the road*, Chaos, **30**(2020), 123115.
- [19] Kumari, S., Chugh, R., Miculescu, R., *On the Complex and Chaotic Dynamics of Standard Logistic Sine Square Map*, An. Stiint. Univ. "Ovidius" Constanta Ser. Mat., **29**(2021), no. 3 (accepted).
- [20] Kumari, S., Chugh, R., Nandal, *A bifurcation analysis of logistic map using four step feedback procedure*, Int. J. Eng. Adv. Tech., **9**(2019), no. 1, 704-707.
- [21] Lo, S.C., Cho, H.J., *Chaos and control of discrete dynamic traffic model*, J. Franklin Inst., **342**(2005), 839-851.
- [22] Lorenz, E.N., *Deterministic nonperiodic lows*, J. Atmos. Sci., **20**(1963), 130-141.
- [23] Mann, W.R., *Mean value methods in iteration*, Proc. Am. Math. Soc., **4**(1953), 506-510.
- [24] May, R., *Simple mathematical models with very complicated dynamics*, Nature, **261**(1976), 459-475.
- [25] Patidar, V., Purohit, G., Sud, K.K., *Dynamical behavior of q deformed Henon map*, Int. J. Bifurc. Chaos, **21**(2011), 1349-1356.
- [26] Patidar, V., Sud, K.K., *A comparative study on the co-existing attractors in the Gaussian map and its q -deformed version*, Commun. Nonlinear Sci. Numer. Simul., **14**(2009), 827-838.
- [27] Prasad, B., Katiyar, K., *Stability and Lyapunov Exponent of a q -deformed map*, Int. J. Pure Appl. Math., **104**(2015), no. 4, 509-516.
- [28] Robinson, C., *Dynamical Systems: Stability, Symbolic Dynamics and Chaos*, CRC Press, Boca Raton, 1995.
- [29] Singh, N., Sinha, A., *Chaos-based secure communication system using logistic map*, Optics and Las. Eng., **48**(2010), 398-404.
- [30] Wiggins, S., *Introduction to Applied Nonlinear Dynamics and Chaos*, Springer, New York, 1990.

Renu Badsiwal
Department of Mathematics,
Maharshi Dayanand University,
Rohtak-124001, Haryana, India
e-mail: renubadsiwal19@gmail.com

Sudesh Kumari
Government College for Girls Sector 14,
Gurugram-122001, Haryana, India
e-mail: tanwarsudesh10@gmail.com

Renu Chugh
Department of Mathematics
Gurugram University, Gurugram-122001, India
e-mail: chugh.r1@gmail.com